Eur. Phys. J. C 35, 537–542 (2004)
Digital Object Identifier (DOI) 10.1140/epjc/s2004-01863-8

THE EUROPEAN PHYSICAL JOURNAL C

An alternate smearing method for Wilson loops in lattice QCD

F. Okiharu[1], R.M. Woloshyn[2]

[1] Department of Physics, Faculty of Science and Technology, Nihon University, 1-8-14 Kanda-Surugadai, Tokyo 1018308, Japan
[2] TRIUMF, 4004 Wesbrook Mall, Vancouver BC, Canada V6T 2A3

Received: 12 February 2004 / Revised version: 7 April 2004 /
Published online: 3 June 2004 –

Abstract. A gauge field link smearing method developed for calculations with staggered fermions, namely the use of unitarized fat7 links, is applied to mesonic and baryonic Wilson loop calculations. This method is found to be very effective for reducing statistical fluctuations for large Wilson loops. Examination of chromo-electric field distributions shows that self-interactions of the static sources are reduced when unitarized fat7 smearing is used but long-distance inter-quark effects are unchanged.

1 Introduction

Wilson loops are used in many applications of lattice QCD, for example, in the study of the static quark potential, string breaking and the chromo-electric and chromo-magnetic field distributions. These calculations can be very challenging for Monte Carlo simulations, because the Wilson loops decrease exponentially with the size of the loop (area law) and rapidly become submerged in statistical fluctuations. Usually some method that will enhance the signal and suppress the noise has to be used. The multihit method [1,2] for reducing the variance of the signal and link smearing which enhances the ground state signal are well known. Also there are special techniques like abelian projection which preserves the essential long-distance physics while removing extraneous random fluctuations (see [3] for a recent application).

The above methods work because they smooth out the gauge fields at distances less than some physically relevant length scale. In other words, the effects of hard gluons, gluons with momenta of the order of the cut-off, are suppressed by some kind of smearing. There is another context in which the suppression of hard gluons is also very important. With staggered fermions on a lattice, so-called species doubling occurs. Multiple copies of staggered fermions (now usually called tastes) exist. During the past few years it has been understood that taste-symmetry breaking, which is a finite lattice spacing artefact, is due to hard gluon interactions [4,5]. Improved staggered fermion actions utilizing fat gauge field links have been developed and have been shown to greatly reduce taste-symmetry breaking [5–7].

It is natural to ask if the methods developed for staggered fermions are also effective in Wilson loop calculations. Indeed it has already been shown that hypercubic blocking, which is used in the so-called HYP action, can reduce the error in static quark–antiquark potential calculations [7].

Recently, further improved staggered fermion actions have been developed [8]. These are based on the idea of unitarized fat7 smearing first discussed by Lee [9]. In the most common smearing method, sometimes called APE smearing [10], one adds to the target link its three link staples with some coefficient and then projects this combination of links back to $SU(3)$. This process is repeated. The relative weighting of the target link and staples and the number of smearing steps are determined essentially by trial and error for different applications. In fat7 smearing one adds not just the three link staples but also five link and seven link staples which extend in mutually orthogonal directions, orthogonal to the direction of the target link [5]. The weighting of the staples is fixed by requirements of action improvement. What has been realized recently is that unitarization or projection to $SU(3)$ is very beneficial for suppression of taste-changing interactions. A nice feature of the unitarized fat7 (Ufat7) scheme is that it is easy implement compared to hypercubic blocking [7]. It is shown here that it is also very effective for Wilson loop calculations.

The fat7 smearing operator involves many more terms than the commonly used APE smearing. For a single smearing of one link, fat7 takes about eight times longer than APE smearing. In typical applications of APE smearing many tens of smearing steps are employed. However, as will be seen from our results, only a few Ufat7 smearing steps are needed to achieve a significant reduction of statistical errors. Therefore, Ufat7 smearing can be used without adversely impacting the overall cost of the calculation.

In Sect. 2 results for the static quark–antiquark potential are presented. Multiple levels of Ufat7 smearing are considered. It is found that the long-distance linearly rising behavior of the potential is preserved by smearing but the Coulomb-like part of the potential at short distances is suppressed. The main effect of smearing is to remove the constant term in the potential. This term is associated with the quark self-energy. A nice way to see how this is

being affected by smearing is to look at the distribution of color field around the static sources. This can be done by calculating the Wilson loop–plaquette correlation [11]. Results for chromo-electric field distributions are presented and with Ufat7 smearing one can see the emergence of a flux tube connecting the static sources even for a fairly small spatial separation.

The baryonic Wilson loop is considered in Sect. 3. This case is much noisier than the mesonic loop. However, aggressive use of Ufat7 smearing is found to reduce statistical errors considerably for the potential at large quark separations compared to the multihit method that has been used before. As with the quark–antiquark potential, the constant term of the potential is essentially removed after a few levels of smearing. Examination of the chromo-electric field distribution shows that self-interaction effects at the static quark sources are highly suppressed by smearing and the inter-quark flux can be revealed.

2 Mesonic Wilson loop

The interaction energy of a static quark–antiquark pair can be determined by taking the large time limit of a Wilson loop $W(R,T)$ of spatial extent R:

$$V(R,T) = -\ln(W(R,T)/W(R,T-1)), \quad (1)$$

$$\to V_{Q\overline{Q}}(R). \quad (2)$$

Both on-axis and off-axis Wilson loops are considered and the static potential is calculated for 24 different quark–antiquark separations up to a maximum separation of 9 lattice units. The numerical simulations were carried out in quenched approximation using the Wilson plaquette action at $\beta = 6.2$ on a 24^4 lattice.

In order to reduce the statistical error some noise reduction technique is commonly used. The multihit method [1,2] has been found to be very effective for static potential calculations. Essentially one integrates out the gauge links in the time direction, replacing them by effective links constructed from the staples attached to the replaced temporal link. In addition, fuzzing or smearing of the links in the spatial segments of the loop is also carried out. This improves the overlap with the ground state and allows the use of (1) at moderate values of T. For the spatial links in the loop, a standard way to do this smearing is to make the replacement [10]

$$U_i(x) \to V = U_i(x) + \alpha \sum_{j \neq i} U_j(x) U_i(x+\widehat{j}) U_j^\dagger(x+\widehat{i}), \quad (3)$$

with the sum on j denoting the sum of staples in spatial directions orthogonal to i. The combination of links is then projected back to $SU(3)$. In this paper we use the projection method in [12] which iteratively finds the element $U' \in SU(3)$which maximizes $\mathrm{ReTr}(U'V^\dagger)$.

In Fig. 1 the static quark–antiquark potential is plotted for a calculation using an ensemble of only eight gauge configurations. The circles in Fig. 1 show the potential (in lattice units) for a standard calculation with multihit and 30 steps for spatial link smearing (3) with $\alpha = 0.15$. The potential obtained using (1) at $T = 8$. The other data sets of Fig. 1 are calculations utilizing one, two or three levels of Ufat7 smearing for all links. In addition to Ufat7 smearing, spatial links are smeared with eight levels of (3) which is sufficient to get good ground state overlap. The decrease of statistical errors achieved with Ufat7 smearing is evident.

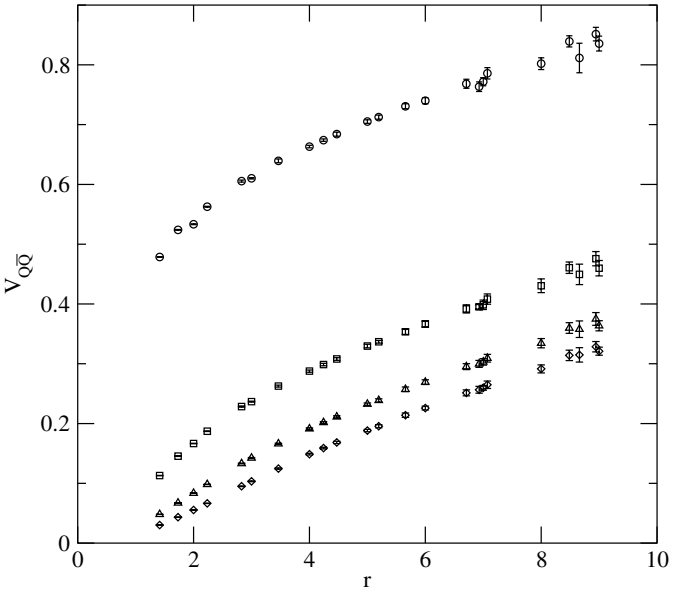

Fig. 1. The static quark–antiquark potential (in lattice units) versus inter-quark separation in a low statistics run. A standard calculation using multihit variance reduction is shown by circles. Results for one, two and three levels of Ufat7 smearing are represented by squares, triangles and diamonds respectively

To investigate how well the long-distance physics is preserved by smearing a high statistics calculation with 1500 gauge configurations was carried out. The potentials are shown in Fig. 2a. The statistical errors are too small to be plotted. In Fig. 2b the different data sets are plotted shifting the points so that the value at $R = 9$ is the same. The long-distance behavior of the potential is preserved remarkably well.

In order to understand what Ufat7 smearing is doing it is useful to look at color field distributions. We calculate the correlation function between the Wilson loop $W(R,T)$ and the plaquette operator $P_{\mu\nu}(x,t)$ given schematically by

$$\frac{\langle WP \rangle}{\langle W \rangle} - \langle P \rangle. \quad (4)$$

Choosing a temporal plaquette P_{i0} yields the square of the chromo-electric field in the ith direction. In the actual calculation the plaquette operator is symmetrized about its spatial base point, that is, the operator $(P_{i0} + P_{-i0})/2$ is used [11]. The temporal position of the plaquette is taken to be at the mid-point of the Wilson loop, $t = T/2$. Using the spatial plaquettes P_{ij} chromo-magnetic fields can also be probed. This was done, but the qualitative features are the same as for chromo-electric fields so no results for chromo-magnetic fields are presented here.

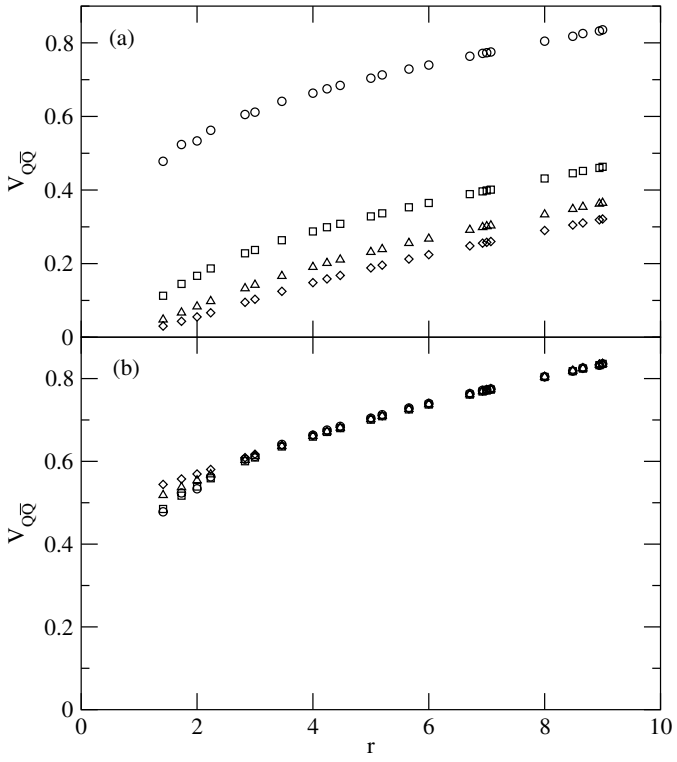

Fig. 2. The static quark–antiquark potential (in lattice units) versus inter-quark separation. A standard calculation using multihit variance reduction is shown by circles. Results for one, two and three levels of Ufat7 smearing are represented by squares, triangles and diamonds respectively. In **b** a constant shift has been applied

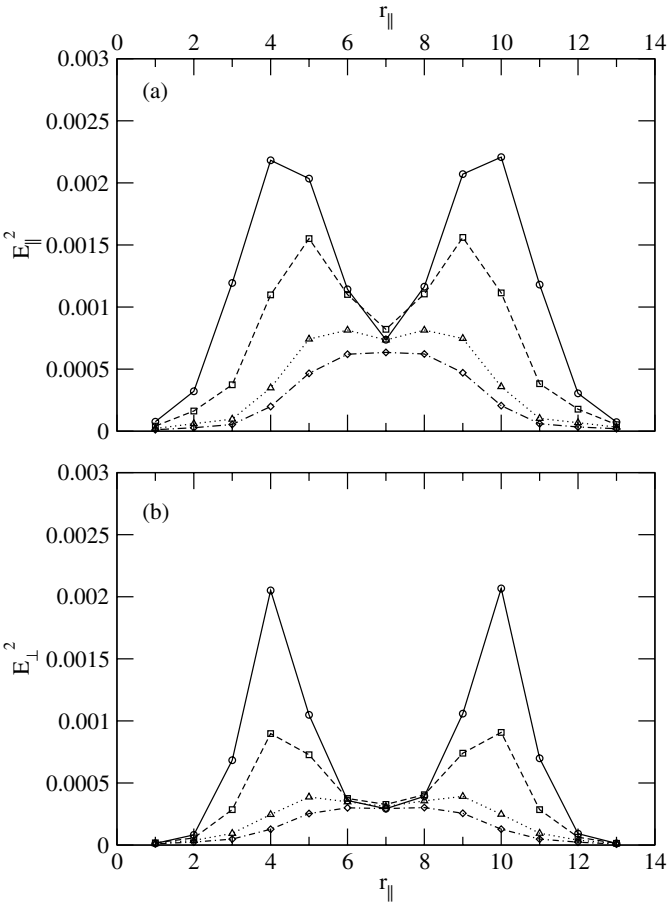

Fig. 3. The square of the chromo-electric field (in lattice units) **a** parallel and **b** perpendicular to the spatial axis of the Wilson loop as a function of the longitudinal coordinate $r_{||}$. The source positions are $r_{||} = 4$ and $r_{||} = 10$

Results are presented for a planar 6×6 Wilson loop. Although this is not a very large loop it is large enough to illustrate the effect of Ufat7 smearing with the advantage that the statistical errors for our high statistics run are small enough to be omitted for the plots. Figure 3 shows the square of the chromo-electric field as a function of the longitudinal coordinate $r_{||}$, the position in the plane of the loop parallel to the spatial segments of the Wilson loop. The field components parallel and transverse to the longitudinal axis are plotted separately. In the coordinate system that was used, the quark and antiquark source positions correspond to $r_{||} = 4$ and $r_{||} = 10$. The circles show the results of a standard calculation, multihit noise reduction for temporal links and standard APE-like smearing of spatial links. For the small loop used here, the flux connecting the quark and antiquark sources is completely submerged in the huge flux that surrounds each source. However, successive levels of Ufat7 remove these short-distance self-interaction effects exposing the nascent flux tube between the sources. This is reenforced by examining the transverse profiles of the E^2 distributions. These are shown in Figs. 4 and 5 for the parallel and transverse field components. The plane of the Wilson loop corresponds to $r_\perp = 5$. After three levels of Ufat7 smearing, the chromo-electric flux outside the Wilson loop is effectively removed, and the transverse profile is essentially the same at all longitudinal positions inside the loop. This is what is expected for confined flux that gives rise to a linearly rising potential.

3 Baryonic Wilson loop

The interactions of three static quarks can be obtained using a three-bladed Wilson loop [3, 13, 14] depicted in Fig. 6. The color indices associated with the three loop segments S_1, S_2 and S_3 are contracted according to

$$W_{3q} = \frac{1}{3!}\epsilon^{abc}\epsilon^{a'b'c'} S_1^{aa'} S_2^{bb'} S_3^{cc'}. \qquad (5)$$

The quark sources are at r_1, r_2, r_3 and the position of the junction point can be chosen arbitrarily, at least, in principle. In practice it may be difficult to achieve the conditions where observables are independent of the shape of the operator used to create and annihilate the three-quark state [15].

To calculate the interaction energy of the three-quark system we use a source and sink where each of the quarks lies on a different spatial axis at a distance l from the origin [13,14]. The junction point of the links connecting the

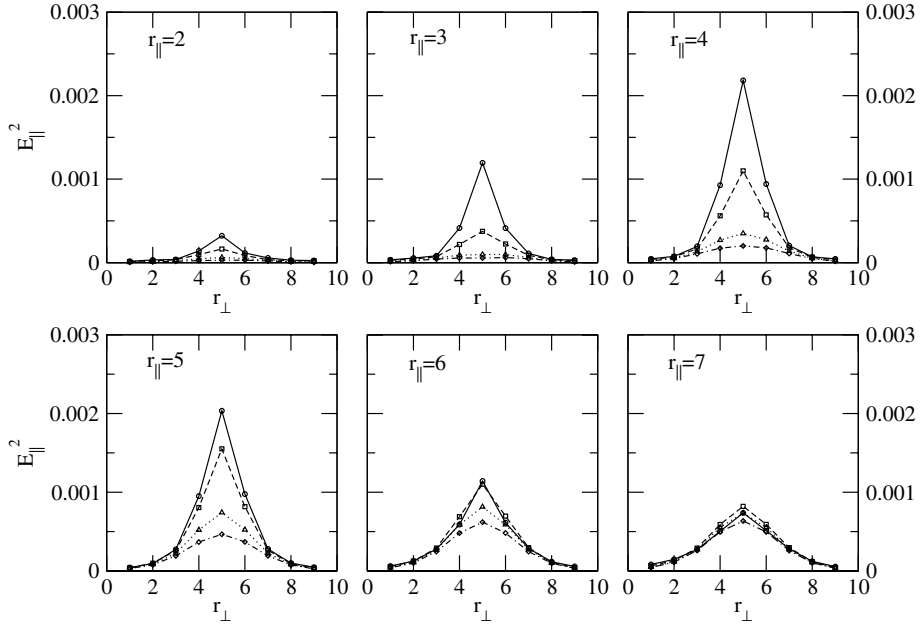

Fig. 4. The profile of the parallel chromo-electric field squared distribution (in lattice units) as a function of position $r_\perp$ transverse to the spatial axis of the loop. The different panels are for different longitudinal positions $r_{||} = 2, 3, 4, 5, 6$ and 7. The source is at $r_{||} = 4,\ r_\perp = 5$

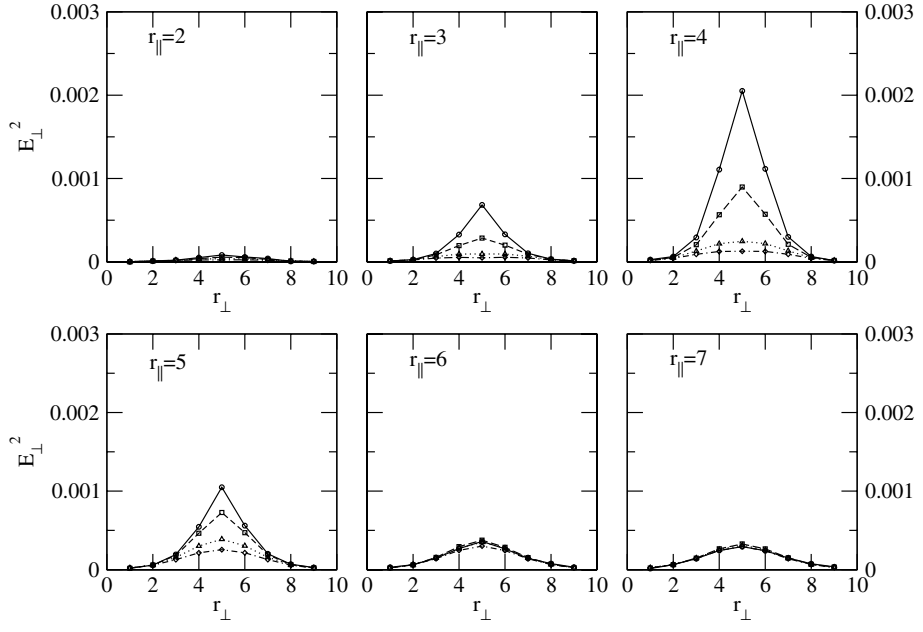

Fig. 5. The profile of the transverse chromo-electric field squared distribution (in lattice units) as a function of position $r_\perp$ transverse to the spatial axis of the loop. The different panels are for different longitudinal positions $r_{||} = 2, 3, 4, 5, 6$ and 7. The source is at $r_{||} = 4,\ r_\perp = 5$

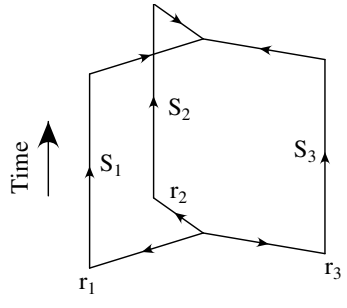

Fig. 6. Three-bladed Wilson loop used for determining the three-quark potential

sources is at the origin. The inter-quark separation is $\sqrt{2}l$ and the sum of the distances from the quark sources to the so-called Steiner point is $\sqrt{3}l$. The three-quark potential is shown in Fig. 7a (circles) for a standard calculation using multihit variance reduction and 40 steps of spatial link smearing. The potential is calculated at $T = 8$ (see (1)) which is sufficient to have a reasonable plateau. Also shown are the potentials with different levels of Ufat7 smearing. The Ufat7 smeared calculations also included spatial link smearing using (3) for 20 steps with $\alpha = 0.25$. In Fig. 7b the results are plotted with a constant shift so that the potentials agree at $l = 6$.

The suppression of statistical fluctuations at large distance is very evident with Ufat7 smearing. The linearly

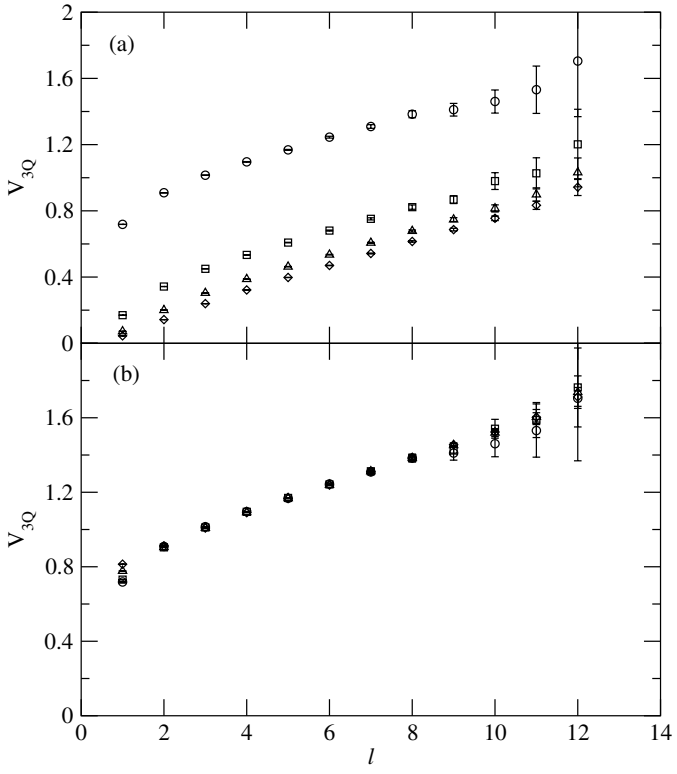

Fig. 7. The static three-quark potential (in lattice units) for a source where each of the quarks lie at a distance l from the origin. A standard calculation using multihit variance reduction is shown by circles. Results for one, two and three levels of Ufat7 smearing are represented by squares, triangles and diamonds respectively. In **b** a constant shift has been applied

rising long-distance behavior is maintained just as in the mesonic case and the main effect is the suppression of the constant potential. This is due to a reduction of the short-distance self-interaction effects at the static sources. Examination of the color field distribution confirms this effect.

The calculation of the flux with a baryonic source is quite challenging so we use a loop with only fairly small separations. The source for this calculation is planar with the shape of a $\top$. The length of the crossarm of the $\top$ is 10 lattice units and the length of the base is 8. The time extent of the loop is 6 with the plaquette probing the flux distribution at time 3. As an example of the flux distribution, Fig. 8 shows $E_{||}^2$, the square of the components of the chromo-electric field in the plane of the baryonic source for different smearings. The scale in each figure is different so that only a qualitative comparison is possible. As Ufat7 smearing is increased, the peaks at the sources are suppressed and the flux connecting the sources becomes visible. This is the same as what was seen in the mesonic case but it seems that more smearing is needed in the baryonic case to achieve a similar level of source suppression.

The behavior of the chromo-electric field is illustrated more quantitatively in Fig. 9. The quantity $E_{||}^2$ (in lattice units) is plotted on a line along the base of the baryonic operator. Recall that the operator has the shape of a $\top$. The point $r = 12$ corresponds to the source point at the bottom of the $\top$ and the point $r = 4$ is the point where the base meets the crossarm. One sees not only the suppression of the self-interaction of the source but also the very significant decrease in the statistical errors achieved through the use of Ufat7 smearing.

The baryonic loop used in the flux distribution measurement is still too small to claim an observation of baryonic flux tubes. However, with a combination of increased statistics, more aggressive Ufat7 smearing and with some tuning of the spatial smearing, it may be possible to go to loops large enough to reveal some interesting features of the color field flux.

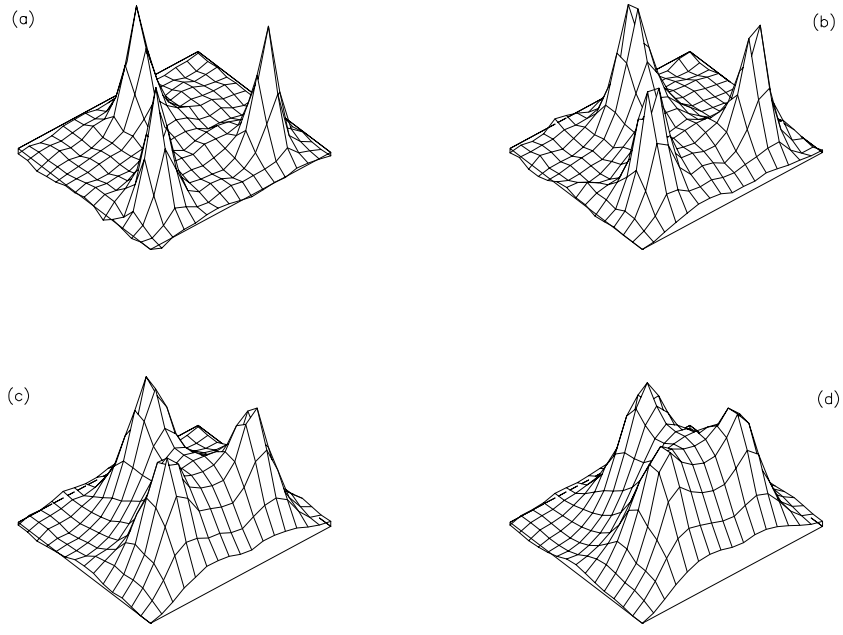

Fig. 8. Surface plot showing the distribution of chromo-electric field squared parallel to the plane of the three-quark source for **a** standard calculation with multihit, **b** one level of Ufat7 smearing, **c** two levels of Ufat7 smearing, **d** three levels of Ufat7 smearing

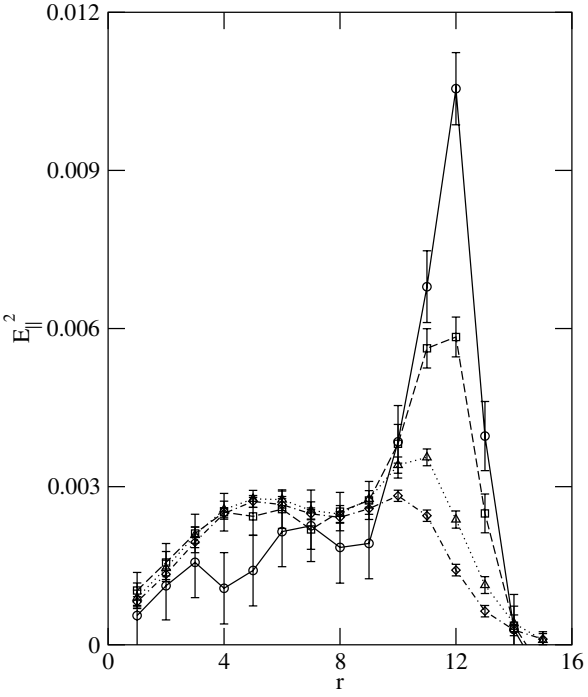

Fig. 9. The square of the chromo-electric field (in lattice units) in the plane of the baryonic operator. The coordinate r is on a line along the base of the operator with the source at $r = 12$

4 Summary

With staggered fermions on a lattice, hard gluons can lead to taste-changing transitions. Recently a strategy using a unitarized fat7 smearing has been developed to reduce these effects in hadrons simulated with staggered quarks. In this work we investigate the use of unitarized fat7 smearing for mesonic and baryonic Wilson loops.

It is found that unitarized fat7 smearing is very effective in reducing statistical errors in large Wilson loops. This comes about because the smearing suppresses short-distance fluctuations associated with self-interaction of the static sources. An indirect manifestation of this suppression is the reduction of the constant term in the potentials as more levels of Ufat7 smearing are applied. The examination of chromo-electric flux distributions shows that large peaks associated with the sources in standard calculations can be removed substantially by using Ufat7 smeared links. The long-distance part of potential and the flux exchanged between sources do not seem to be disturbed by the smearing.

The fact that a method developed to suppress hard gluon interactions of staggered quarks also works well for Wilson loops encourages us to think that relevant physical effects have been identified and controlled. It is hoped that unitarized fat7 smearing will find useful applications where large Wilson loops are calculated.

Acknowledgements. This work is supported in part by the Natural Sciences and Engineering Research Council of Canada.

References

1. G. Parisi, R. Petronzio, F. Rapuano, Phys. Lett. B **128**, 418 (1983)
2. Ph. de Forcrand, C. Roiesnel, Phys. Lett. B **151**, 77 (1985)
3. H. Ichie, V. Bornyakov, T. Streuer, G. Schierholz, Nucl. Phys. Proc. Suppl. **119**, 751 (2003)
4. G.P. Lepage, Phys. Rev. D **59**, 074502 (1999)
5. K. Orginos, D. Toussaint, R.L. Sugar, Phys. Rev. D **60**, 054503 (1999)
6. T. Blum, C. DeTar, S. Gottlieb, K. Rummukainen, U.M. Heller, J.E. Hetrick, D. Toussaint, R.L. Sugar, M. Wingate, Phys. Rev. D **55**, 1133 (1997)
7. A. Hasenfratz, F. Knechtli, Phys. Rev. D **64**, 034504 (2001)
8. HPQCD Collaboration, E. Follana et al., hep-lat/0311004
9. W. Lee, Phys. Rev. D **66**, 114504 (2002)
10. APE Collaboration, M. Albanese et al., Phys. Lett. B **192**, 103 (1987)
11. G. Bali, K. Schilling, Ch. Schlichter, Phys. Rev. D **51**, 5165 (1995)
12. J. Hoek, Nucl. Phys. B **329**, 240 (1990)
13. T.T. Takahasi, H. Matsufuru, Y. Nemoto, H. Suganuma, Phys. Rev. Lett. **65**, 18 (2001)
14. C. Alexandrou, Ph. de Forcrand, A. Tsapalis, Phys. Rev. D **65**, 054503 (2002)
15. F. Okiharu, R.M. Woloshyn, hep-lat/0310007